Topological condensate in an interaction-induced gauge potential

Jun-hui Zheng,[1] Bo Xiong,[1] Gediminas Juzeliūnas,[2] and Daw-Wei Wang[1,3]
[1]*Department of Physics, National Tsing Hua University, Hsinchu, Taiwan*
[2]*Institute of Theoretical Physics and Astronomy, Vilnius University, A. Goštauto 12, Vilnius 01108, Lithuania*
[3]*Physics Division, National Center for Theoretical Sciences, Hsinchu, Taiwan*
(Received 2 December 2014; revised manuscript received 9 June 2015; published 2 July 2015)

We systematically investigate the ground-state and elementary excitations of a Bose-Einstein condensate within a synthetic vector potential, which is induced by the many-body effects and atom-light coupling. For a sufficiently strong spin-dependent interaction, we find the condensate undergoes a Stoner-type ferromagnetic transition through the self-consistent coupling with the vector potential. For a weak interaction, the critical velocity of a supercurrent is anisotropic due to the density fluctuations affecting the gauge field. We further analytically demonstrate the topological ground state with a coreless vortex ring in a three-dimensional (3D) harmonic trap and a coreless vortex-antivortex pair in a two-dimensional (2D) trap. The circulating persistent current is measurable in the time-of-flight experiment or in the dipolar oscillation through the violation of the Kohn theorem.

DOI: 10.1103/PhysRevA.92.013604 PACS number(s): 67.85.−d, 03.75.Lm, 03.75.Mn, 11.15.Kc

I. INTRODUCTION

Gauge fields play an important role in modern particle physics, mediating interaction between elementary particles. In condensed-matter physics, the gauge fields bring many important phenomena, such as integer and factional quantum Hall effects [1,2], Laughlin liquids [3], and the Hofstadter butterfly spectrum [4]. In quantum gas systems, artificial gauge fields can be also generated for neutral atoms in the rotating frame [5,6] or by the atom-light coupling with spatially dependent laser fields [7–9] or detuning [10,11]. This opens up new possibilities to study many-body physics with gauge potential and is extended to investigate the spin-orbital (SO) coupling problems in similar experiments [12]. Note that the synthetic magnetic field experiment [10] and spin-orbital system [12,13] are in two opposite parameter regimes: The former requires the recoiled energy to be much smaller than the energy separation between the dressed states (set by the strength of Raman laser), so the BEC occupies in the lowest-energy state with an effective magnetic field via the adiabatic approximation. On the other hand, the SO-coupled condensate requires a smaller Raman laser in order to include all the spin degrees of freedom.

Besides these schemes, it was theoretically proposed to have gauge potentials induced by dipole-dipole interaction [14–16] or by regular contact interaction through the inhomogenous condensate density, while only condensate dynamics [17] and excitations [18] in a one-dimensional (1D) system have been investigated so far. Since the mean-field solution can be easily destroyed by the finite-temperature effects and quantum fluctuations in 1D, it is more realistic and demanding to investigate many-body properties in higher dimensional systems, where the effective gauge field may further introduce topological defects and more interesting many-body physics not observable in 1D systems.

In this paper, we systematically investigate the ground state and excitation properties of a (pseudo)-spin-1/2 condensate with the *interaction-induced* gauge field in higher dimensional (2D and 3D) systems. To highlight a difference of such a gauge field from the previously considered ones [7–11] induced by spatially dependent laser fields, in this paper only a uniform laser field is considered, so that no effective magnetic field emerges if no interaction effects are considered. The effective equations of motion are therefore derived self-consistently through the interaction effects, which allow us to go beyond the perturbative regime studied before [17]. Several interesting many-body properties are highlighted here: (i) The condensate can undergo a Stoner-type ferromagnetism self-consistently through an interplay between the interaction and the synthetic field; i.e., the relative amplitude of the two components of spinor in the coherent ground state can be changed sharply when the interaction is larger than a critical value. However, due to the spin-dependent interaction, the ferromagnetism is to break $U(1)\times Z_2$ symmetry instead of the SU(2) symmetry in fermionic case. (ii) In the weak interaction limit of a uniform space, the critical velocity for the energetic instability becomes anisotropic in space due to the density fluctuations within the gauge potential. (iii) In a harmonic trap, we show both analytically and numerically that the ground state has a coreless vortex ring around the gauge field in a 3D trap and a coreless vortex-antivortex pair in a 2D trap. Such topological structure, which reflects the nonuniform particle density distribution, is strong evidence of the many-body interaction effect on the synthetic gauge field. (iv) We further discuss how the topological condensate can be measured in the time-of-flight experiment and/or in the dipolar oscillation, where the Kohn theorem [19,20] fails due to the interaction-induced gauge potential.

The article is organized as follows. In Sec. II, we introduce the Hamiltonian for the system considered, and then derive a two-component Gross-Pitaevskii (GP) equation, which can be furthermore simplified to a one-component GP equation under adiabatic approximation. In Sec. III, we list the main results in uniform space, such as the Stoner-type ferromagnetism in the strong interaction limit and analysis of the critical velocity in the weak interaction limit. In Sec. IV, we show the topological ground state in a trapped system. In Sec. V, we discuss methods to measure the topological condensate proposed in this paper. In Sec. VI, we give a brief summary of the results.

II. SYSTEM HAMILTONIAN AND ITS MEAN-FIELD EQUATION

In this article, we consider bosonic atoms with two internal states subjected to a Raman coupling. Within the rotating-wave approximation, the Hamiltonian can be expressed as $\hat{H} = \sum_{i=1}^{N} \hat{H}_1(i) + \sum_{i<j}^{N} \hat{H}_2(i,j)$, where the single-particle Hamiltonian is ($\hbar \equiv 1$)

$$\hat{H}_1 = \frac{\mathbf{p}^2}{2m}\hat{\mathbf{I}} + \frac{1}{2}\begin{bmatrix} \Delta & \Omega\, e^{-2i\mathbf{k}_r\cdot\mathbf{r}} \\ \Omega\, e^{2i\mathbf{k}_r\cdot\mathbf{r}} & -\Delta \end{bmatrix} + V_{\rm trap}(\mathbf{r})\hat{\mathbf{I}}, \quad (1)$$

with $\mathbf{k}_r$ being the recoil momentum and $V_{\rm trap}(\mathbf{r})$ being the spin-independent trapping potential. The two-body interaction may be spin dependent and long ranged in general, $H_2^{\sigma\sigma'} = V_{\sigma\sigma'}(\mathbf{r}_i - \mathbf{r}_j)$, with $\sigma,\sigma' = \uparrow/\downarrow$ being the pseudospin indices. For simplicity, we just consider a spatially *independent* detuning Δ and Rabi frequency Ω. After the second quantization, the total Hamiltonian becomes $\hat{H} = \sum_{\sigma,\sigma'} \int d\mathbf{r}\hat{\Psi}_\sigma^\dagger(\mathbf{r}) H_1^{\sigma\sigma'} \hat{\Psi}_{\sigma'}(\mathbf{r}) + \frac{1}{2}\sum_{\sigma,\sigma'} \int d\mathbf{r}d\mathbf{r}' \hat{\Psi}_\sigma^\dagger(\mathbf{r})\hat{\Psi}_{\sigma'}^\dagger(\mathbf{r}') V_{\sigma\sigma'}(\mathbf{r}-\mathbf{r}')\hat{\Psi}_{\sigma'}(\mathbf{r}')\hat{\Psi}_\sigma(\mathbf{r})$, where $\hat{\Psi}_\sigma(\mathbf{r})$ is the bosonic field operator. Although the above Hamiltonian is the same as the ones to study the SO-coupled condensate (see, for example, Refs. [12,21]), we will concentrate on the adiabatic regime, $\Omega \gg E_r = k_r^2/2m$, where only one dressed-state component is involved.

A. Two-component GP equation

In the following, we deduce the two-component GP equation, which is intrinsically a single-particle-like equation of motion (EOM) with a mean-field contribution. Considering many-body properties at zero temperature, we can approximate the ground state $|G\rangle$ by a coherent state wave function, i.e., $\hat{\Psi}_\sigma(\mathbf{r})|G\rangle = \Phi_\sigma(\mathbf{r})|G\rangle$, where $\Phi_\sigma(\mathbf{r})$ is the condensate wave function normalized to the total number of particles, i.e., $\sum_\sigma \int \Phi_\sigma^\dagger(\mathbf{r})\Phi_\sigma(\mathbf{r})d\mathbf{r} = N$. Then the mean-field energy $E \equiv \langle G|\hat{H}|G\rangle$ reads

$$\begin{aligned} E = &\sum_{\sigma\sigma'} \int d\mathbf{r}\Phi_\sigma^* H_1^{\sigma\sigma'} \Phi_{\sigma'} \\ &+ \frac{1}{2}\int d\mathbf{r}d\mathbf{r}' |\Phi_\uparrow(\mathbf{r})|^2 |\Phi_\uparrow(\mathbf{r}')|^2 V_{\uparrow\uparrow}(\mathbf{r}-\mathbf{r}') \\ &+ \frac{1}{2}\int d\mathbf{r}d\mathbf{r}' |\Phi_\downarrow(\mathbf{r})|^2 |\Phi_\downarrow(\mathbf{r}')|^2 V_{\downarrow\downarrow}(\mathbf{r}-\mathbf{r}') \\ &+ \int d\mathbf{r}d\mathbf{r}' |\Phi_\uparrow(\mathbf{r})|^2 |\Phi_\downarrow(\mathbf{r}')|^2 V_{\uparrow\downarrow}(\mathbf{r}-\mathbf{r}'). \end{aligned} \quad (2)$$

By requiring the variation of the action with respect to $\Phi_\sigma(\mathbf{r})$ to be zero, i.e., $\frac{\delta}{\delta\Phi_\sigma}\langle G|\sum_\sigma i\hat{\Psi}_\sigma^*\partial_t\hat{\Psi}_\sigma - \hat{H}|G\rangle = 0$, we arrive at the two-component GP equation,

$$i\partial_t\begin{pmatrix}\Phi_\uparrow \\ \Phi_\downarrow\end{pmatrix} = H_1\begin{pmatrix}\Phi_\uparrow \\ \Phi_\downarrow\end{pmatrix} + \begin{pmatrix} G_1 & 0 \\ 0 & G_2\end{pmatrix}\begin{pmatrix}\Phi_\uparrow \\ \Phi_\downarrow\end{pmatrix}, \quad (3)$$

where

$$G_1(\mathbf{r}) = \int d\mathbf{r}'[|\Phi_\uparrow(\mathbf{r}')|^2 V_{\uparrow\uparrow}(\mathbf{r}_\Delta) + |\Phi_\downarrow(\mathbf{r}')|^2 V_{\uparrow\downarrow}(\mathbf{r}_\Delta)],$$

$$G_2(\mathbf{r}) = \int d\mathbf{r}'[|\Phi_\downarrow(\mathbf{r}')|^2 V_{\downarrow\downarrow}(\mathbf{r}_\Delta) + |\Phi_\uparrow(\mathbf{r}')|^2 V_{\uparrow\downarrow}(\mathbf{r}_\Delta)],$$

with $\mathbf{r}_\Delta = \mathbf{r} - \mathbf{r}'$. By expressing the matrix $\mathrm{diag}(G_1, G_2)$, a linear combination of Pauli matrices, Eq. (3) becomes

$$i\partial_t\begin{pmatrix}\Phi_\uparrow \\ \Phi_\downarrow\end{pmatrix} = H_1\begin{pmatrix}\Phi_\uparrow \\ \Phi_\downarrow\end{pmatrix} + \left(\frac{Q}{2} + \frac{G}{2}\sigma_z\right)\begin{pmatrix}\Phi_\uparrow \\ \Phi_\downarrow\end{pmatrix}, \quad (4)$$

with

$$Q = G_1 + G_2,\ G = G_1 - G_2. \quad (5)$$

Thus the single-particle-like effective Hamiltonian is

$$\begin{aligned} \hat{H}_1^{\rm eff} &\equiv H_1 + \frac{Q}{2} + \frac{G}{2}\sigma_z \\ &= \left[\frac{\mathbf{p}^2}{2m} + V_{\rm trap} + \frac{Q}{2}\right]\hat{\mathbf{I}} + \frac{1}{2}\begin{bmatrix} \tilde{\Delta}(\mathbf{r}) & \Omega\, e^{-2i\mathbf{k}_r\cdot\mathbf{r}} \\ \Omega\, e^{2i\mathbf{k}_r\cdot\mathbf{r}} & -\tilde{\Delta}(\mathbf{r}) \end{bmatrix} \end{aligned} \quad (6)$$

with an effective detuning shifted by the interaction,

$$\tilde{\Delta}(\mathbf{r}) = \Delta + G(\mathbf{r}), \quad (7)$$

and an effective trap $\tilde{V}_{\rm trap}(\mathbf{r}) = V_{\rm trap}(\mathbf{r}) + Q(\mathbf{r})/2$.

B. Interaction-induced synthetic gauge field (adiabatic approximation)

We want to diagonalize the Hamiltonian (6) within Born-Oppenheimer approximation (BOA) and then use adiabatic approximation to get an effective single-component GP equation. The spatially uniform Raman coupling (which means Ω, Δ are constants here) considered above should *not* provide any synthetic magnetic field for a noninteracting system (see Refs. [7–11]). However, as we will show, the additional position-dependent detuning term $G(\mathbf{r})$ due to interparticle interaction can contribute an effective magnetic field so that the gauge field and dressed state can be mixed by a self-consistent equation. In order to investigate such new physics, we first omit the kinetic term under BOA and diagonalize the rest parts of $\hat{H}_1^{\rm eff}$ through a spatially dependent transformation,

$$S(\mathbf{r}) = \frac{1}{\sqrt{2}}\begin{bmatrix} e^{i\mathbf{k}_r\cdot\mathbf{r}}\sqrt{1+\tilde{\Delta}/\Lambda} & e^{-i\mathbf{k}_r\cdot\mathbf{r}}\sqrt{1-\tilde{\Delta}/\Lambda} \\ -e^{i\mathbf{k}_r\cdot\mathbf{r}}\sqrt{1-\tilde{\Delta}/\Lambda} & e^{-i\mathbf{k}_r\cdot\mathbf{r}}\sqrt{1+\tilde{\Delta}/\Lambda} \end{bmatrix}, \quad (8)$$

where $\Lambda(\mathbf{r}) = \sqrt{\tilde{\Delta}(\mathbf{r})^2 + \Omega^2}$ and the $\mathbf{r}$ dependence is mostly suppressed for convenience. In the frame of the basis $\tilde{\Phi}(\mathbf{r}) (= [\tilde{\Phi}_+(\mathbf{r}), \tilde{\Phi}_-(\mathbf{r})]^T \equiv S(\mathbf{r})\cdot\Phi(\mathbf{r}))$, the EOM becomes $i\partial_t\tilde{\Phi} = \frac{(-i\nabla - iS\nabla S^\dagger)^2}{2m}\tilde{\Phi} + [V_{\rm trap} + \frac{Q}{2} + \frac{\Lambda}{2}\sigma_z]\tilde{\Phi}$, where the gauge field is given by $-iS\nabla S^\dagger = \frac{\Omega}{\Lambda}\mathbf{k}_r\sigma_x + \frac{\Omega\nabla\tilde{\Delta}}{2\Lambda^2}\sigma_y - \frac{\tilde{\Delta}}{\Lambda}\mathbf{k}_r\sigma_z$.

Within the standard adiabatic approximation [8], the effect of the off-diagonal tunneling terms in the new EOM above can be neglected (after expanding the kinetic energy term) when the recoil energy $E_r = k_r^2/2m$ and the Doppler shift kk_r/m are small compared to the Rabi frequency Ω. Thus, the new EOM decouples into two individual single-component GP equations:

$$\begin{aligned} i\partial_t\tilde{\Phi}_\pm = &\frac{1}{2m}\left(-i\nabla \mp \frac{\tilde{\Delta}}{\Lambda}\mathbf{k}_r\right)^2\tilde{\Phi}_\pm + V_{\rm trap}(\mathbf{r})\tilde{\Phi}_\pm + \frac{Q}{2}\tilde{\Phi}_\pm \\ &\pm\frac{\Lambda}{2}\tilde{\Phi}_\pm + \frac{1}{8m}\frac{\Omega^2}{\Lambda^2}\left[\frac{(\nabla\tilde{\Delta})^2}{\Lambda^2} + 4\mathbf{k}_r^2\right]\tilde{\Phi}_\pm. \end{aligned} \quad (9)$$

Without considering the interaction effect, $\tilde{\Delta}$ recovers to Δ, and then $\tilde{\Delta}\mathbf{k}_r/\Lambda$ is just a momentum shift without any synthetic magnetic field. Throughout this paper, we will assume that the condensate is initially prepared in the lower branch ($\tilde{\Phi}_-$) state and remains there without involving the higher energy branch (since the off-diagonal term is negligible). Therefore, the total density is $\rho(\mathbf{r}) = |\tilde{\Phi}_-(\mathbf{r})|^2$, and the densities in original spin states are $\rho_\uparrow(\mathbf{r}) = |S_{21}(\mathbf{r})|^2\rho(\mathbf{r})$ and $\rho_\downarrow(\mathbf{r}) = |S_{22}(\mathbf{r})|^2\rho(\mathbf{r})$, respectively. Note that it is very different from Refs. [22–24], in which the authors considered the interaction effect for a pure Rashba-type or equal Rashba-Dresselhaus-type spin-orbital system in a relatively smaller Ω region, and did not deal with the dynamical gauge fields. Even though the system we consider is the same as that in Ref. [17], where the authors first obtain the adiabatic basis through a perturbative method and subsequently derive the effective Hamiltonian, the method developed here is based on a self-consistent approach valid for both weak and strong interaction regimes.

In this paper, we just consider the short-ranged interaction between atoms, i.e., $V_{\sigma\sigma'}(\mathbf{r}-\mathbf{r}') = g_{\sigma\sigma'}\delta(\mathbf{r}-\mathbf{r}')$ with $g_{\sigma\sigma'} = 4\pi a_{\sigma\sigma'}/m$, where $a_{\sigma\sigma'}$ is the spin-dependent s-wave scattering length. Through substituting the above $\rho_\uparrow$ and $\rho_\downarrow$, the additional detuning term $G(\mathbf{r})$ is found to satisfy the self-consistent equation

$$G(\mathbf{r}) = \frac{\rho(\mathbf{r})}{2}\left[g_a - g_{as}\frac{\tilde{\Delta}(\mathbf{r})}{\Lambda(\mathbf{r})}\right], \tag{10}$$

where $g_a = g_{\uparrow\uparrow} - g_{\downarrow\downarrow}, g_s = (g_{\uparrow\uparrow} + g_{\downarrow\downarrow} + 2g_{\uparrow\downarrow})/4$, and $g_{as} = (g_{\uparrow\uparrow} + g_{\downarrow\downarrow} - 2g_{\uparrow\downarrow})$. It is worth stressing that $\tilde{\Delta} = \Delta + G$ and $\Lambda = \sqrt{\tilde{\Delta}^2 + \Omega^2}$ are also functions of G. Similarly, the effective potential shift is found to be $Q(\mathbf{r}) = \frac{\rho(\mathbf{r})}{2}[4g_s - g_a\frac{\tilde{\Delta}(\mathbf{r})}{\Lambda(\mathbf{r})}]$. The numerical solution is obtained by the imaginary time evolution method to solve Eq. (9) starting from an "arbitrary" wave function and finding the self-consistent $G(\mathbf{r})$ through Eq. (10) at each step. This method can be easily extended to the long-range case where the right-hand side of Eq. (10) becomes a functional of $G(\mathbf{r})$ and $\rho(\mathbf{r})$.

III. RESULTS IN UNIFORM SPACE

A. Ferromagnetism in the strong interaction limit

A general solution of the detuning shift $G(\mathbf{r})$ can be obtained in a uniform system for Eq. (10). Defining $\sinh\theta = \tilde{\Delta}/\Omega$ (i.e., $\cosh\theta = \Lambda/\Omega$), Eq. (10) becomes

$$F[\theta] \equiv \sinh\theta + B\tanh\theta = C, \tag{11}$$

where $B = g_{as}\rho/2\Omega$ and $C = (\Delta + g_a\rho/2)/\Omega$. Equation (11) has different types of solutions in the following two regimes (see Fig. 1): Case I: When $B > -1$, or when $B < -1$ but $|C| > C_*$, only one solution is available, where $C_* \equiv F[\cosh^{-1}(|B|^{1/3})]$ is the critical value. Especially for the weak interacting case ($|B|, |C| \ll 1$), both θ and $\tanh\theta = \tilde{\Delta}/\Lambda$ are small, so that the $G(\mathbf{r}) \approx g_a\rho(\mathbf{r})/2$ and $Q(\mathbf{r}) \approx 2g_s\rho(\mathbf{r})$. Case II: When $B < -1$ and $|C| < C_*$, there are three solutions and only one of them is the true ground state with the lowest energy.

Taking the zero detuning case ($\Delta = 0$) for simplicity, the chemical potential can be easily obtained from Eq. (9): $\mu = (Q - \Lambda)/2 + E_r\Omega^2/\Lambda^2 = g_s\rho - \frac{1}{2}\Omega(C\tanh\theta + \cosh\theta) + E_r/\cosh^2\theta$. The result shows the

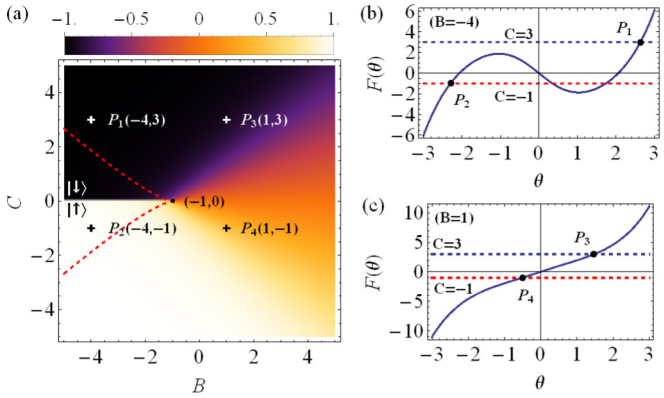

FIG. 1. (Color online) (a) Density plot of magnetization, $M_\chi = (\rho_\uparrow - \rho_\downarrow)/\rho$, as a function of $B = g_{as}/2\Omega$ and $C = g_a/2\Omega$ for zero detuning ($\Delta = 0$). The regime between red (gray) dashed lines has three solutions of θ (case II, see the text). Panels (b) and (c) show the function $F[\theta]$ [solid lines; see Eq. (11)] and the values of C (horizontal dashed lines) for different positions P_i ($i = 1, \ldots, 4$) in panel (a). The ground state of each P_i is denoted by the filled circle.

one corresponding to the largest $|\theta|$ in the three solutions has the minimum chemical potential. Consequently, we may define the magnetization $M_\chi \equiv (\rho_\uparrow - \rho_\downarrow)/\rho = |S_{21}|^2 - |S_{22}|^2 = -\tilde{\Delta}/\Lambda = -\tanh\theta$ as an order parameter and find that M_χ is discontinuous at $C = 0$ as $B < -1$. Since $C \propto g_a = 0$ represents a $U(1) \times Z_2$ symmetry without a "magnetic field" imbalance, the critical change in the magnetization along the $C = 0$ line can therefore be regarded as a Stoner-type ferromagnetism. In Fig. 1, we show the value of M_χ in the $B - C$ diagram by setting $\Delta = 0$. We note that such a phase transition merely occurs in a regime of rather strong interaction, i.e., $|g_{as}|\rho \gtrsim 2\Omega \gg E_r$. For the ^{87}Rb atom, taking typical parameters $\Omega = 2\pi \times 10\,\text{kHz}$ and $\rho = 5 \times 10^{14}\,\text{cm}^{-3}$, it requires $a_{\uparrow\downarrow} - a_{\uparrow\uparrow} - a_{\downarrow\downarrow} > 13.7\,\text{nm}$. This may be achievable using the Feshbach resonance or confinement resonance between two pseudospin states. The Stoner-type phase transition is similar to the phase separation of a two-component condensate, but the two components are now coherently combined together by the Raman coupling.

B. Excitations and energetic instability of superfluid current (weak interaction limit)

Now we investigate the condensate in a uniform space in the weak interaction limit ($|g_{a,as,s}|\rho(\mathbf{r}) \ll \Omega$) at zero detuning, which implies $|B| \ll 1$ and $|C| \ll 1$. From the analysis in case I, we have $G(\mathbf{r}) = g_a\rho(\mathbf{r})/2$ and $Q(\mathbf{r}) = 2g_s\rho(\mathbf{r})$ in the leading order, which also implies $\Lambda = \sqrt{(\Delta + G)^2 + \Omega^2} \approx \Omega$. Using the fact $(\frac{\nabla\tilde{\Delta}}{\Lambda})^2 \ll 4\mathbf{k}_r^2$ [17], the lower branch in Eq. (9) can be simplified to be

$$i\hbar\partial_t\psi = \frac{\hbar^2}{2m}(-i\nabla + \mathbf{a}\rho)^2\psi + b\rho\psi, \tag{12}$$

where $\mathbf{a} = g_a\mathbf{k}_r/2\Omega$ and $b = g_s$. In this process, we have neglected the constant term and denote $\psi(\mathbf{r}) = \tilde{\Phi}_-(\mathbf{r})$ for convenience. Equation (12) is consistent with the 1D result of Ref. [17] to the leading order of weak interaction. For a general wave function $\psi = \sqrt{\rho}e^{i\eta}$, the superfluid velocity is

$\mathbf{v}(\mathbf{r}) = \frac{1}{m}(\nabla\eta + \mathbf{a}\rho)$ due to the effect of gauge field and the corresponding Hydrodynamic equations are

$$\partial_t \rho = -\nabla \cdot (\rho \mathbf{v}), \tag{13}$$

$$\partial_t \eta = -\left(-\frac{1}{2m\sqrt{\rho}}\nabla^2\sqrt{\rho} + \frac{m\mathbf{v}^2}{2} + b\rho\right). \tag{14}$$

We start from the state $\psi_0(\mathbf{r},t) = \sqrt{\rho_0}e^{i\eta_0}$ with $\eta_0 = m\mathbf{v}_g \cdot \mathbf{r} - \mu_0 t$, which is spatially uniform and carries a constant superfluid velocity, $\mathbf{v}_s = \mathbf{v}_g + \mathbf{a}\rho_0/m$. The corresponding chemical potential is $\mu_0 = \frac{m\mathbf{v}_s^2}{2} + b\rho_0$ from Eq. (14). In the following, we consider the fluctuation of the wave function around the static solution, i.e.,

$$\rho = \rho_0 + \delta\rho, \tag{15}$$

$$\eta = \eta_0 + \delta\eta, \tag{16}$$

$$m\mathbf{v} = m\mathbf{v}_s + \nabla\delta\eta + \mathbf{a}\delta\rho. \tag{17}$$

It is easy to find $m\delta\mathbf{v} = \nabla\delta\eta + \mathbf{a}\delta\rho$ from Eq. (17). Thus, the linear perturbative expansion of Eq. (13) is

$$\partial_t\delta\rho = -\nabla\delta\rho \cdot \mathbf{v}_s - \frac{\rho_0}{m}(\nabla^2\delta\eta + \mathbf{a}\cdot\nabla\delta\rho), \tag{18}$$

which shows that the Laplace of $\delta\eta$ satisfies

$$\nabla^2\delta\eta = -\nabla\delta\rho \cdot \frac{m\mathbf{v}_s}{\rho_0} - \frac{m\partial_t\delta\rho}{\rho_0} - \mathbf{a}\cdot\nabla\delta\rho. \tag{19}$$

Similarly, the perturbative expansion of Eq. (14) reads

$$\partial_t\delta\eta = -\left(-\frac{1}{4m\rho_0}\nabla^2\delta\rho + m\mathbf{v}_s\cdot\delta\mathbf{v} + b\delta\rho\right). \tag{20}$$

By performing the time derivation of Eq. (19) and use it to subtract the Laplace of Eq. (20), i.e., $\partial_t(19) - \nabla^2(20)$, then we obtain

$$\frac{(\nabla^2)^2}{4m\rho_0}\delta\rho - \mathbf{v}_s\cdot(\nabla\nabla^2\delta\eta + \mathbf{a}\nabla^2\delta\rho) - b\nabla^2\delta\rho = -\partial_t\nabla\delta\rho\cdot\frac{m\mathbf{v}_s}{\rho_0} - \frac{m\partial_t^2\delta\rho}{\rho_0} - \mathbf{a}\cdot\partial_t\nabla\delta\rho, \tag{21}$$

where we have used the fact $m\delta\mathbf{v} = \nabla\delta\eta + \mathbf{a}\delta\rho$. Now substitute Eq. (19) into Eq. (21) to cancel $\nabla^2\eta$, and we get the differential equation of $\delta\rho$,

$$\begin{aligned} -\partial_t^2\delta\rho - 2\mathbf{v}_s\cdot\partial_t\nabla\delta\rho - \frac{\mathbf{a}\rho_0}{m}\cdot\partial_t\nabla\delta\rho \\ = \frac{(\nabla^2)^2}{4m^2}\delta\rho - \frac{b\rho_0}{m}\nabla^2\delta\rho - \frac{\mathbf{v}_s\cdot\mathbf{a}\rho_0}{m}\nabla^2\delta\rho \\ + (\mathbf{v}_s\cdot\nabla)^2\delta\rho + (\mathbf{v}_s\cdot\nabla)\left(\frac{\mathbf{a}\rho_0}{m}\cdot\nabla\right)\delta\rho. \end{aligned} \tag{22}$$

By substituting $\delta\rho \propto \exp(-i\omega_{\mathbf{k}}t + i\mathbf{k}\cdot\mathbf{r})$ into Eq. (22), we find the the excitation spectrum,

$$\omega_{\mathbf{k}} = \mathbf{k}\cdot(\mathbf{v}_s + \mathbf{v}_a) + \sqrt{(c^2 + 2\mathbf{v}_s\cdot\mathbf{v}_a + (\mathbf{v}_a\cdot\hat{k})^2)\mathbf{k}^2 + \frac{\mathbf{k}^4}{4m^2}}, \tag{23}$$

where $c \equiv \sqrt{b\rho_0/m}$ and $\mathbf{v}_a = \frac{\mathbf{a}\rho_0}{2m}$. Especially in the absence of the gauge field, i.e., $\mathbf{v}_a = 0$, we have $\omega_{\mathbf{k}} = \mathbf{v}_s\cdot\mathbf{k} + \sqrt{c^2\mathbf{k}^2 + \mathbf{k}^4/4m^2}$, which recovers to the conventional BEC with the standard Landau critical velocity c.

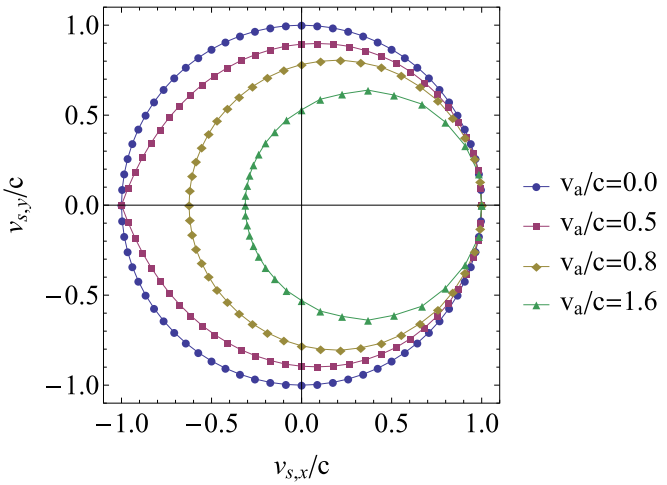

FIG. 2. (Color online) The critical velocity for different ratio v_a/c, where $\mathbf{v}_a = g_a\rho_0\mathbf{k}_r/4\Omega m$ is along the x axis. The superfluid is stable inside the circle.

When the gauge field is finite, it is convenient to denote $\mathbf{v}_a = v_a(1,0,0)$ and $\mathbf{v}_s = v_s(\cos\xi, \sin\xi, 0)$ without loss of generality, where ξ represents the angle between superfluid velocity and light. For the superfluid to be stable, it requires that for every fixed $\mathbf{v}_s$, the excitation $\omega_{\mathbf{k}} > 0$ for all $\mathbf{k} = k(\sin\gamma\cos\kappa, \sin\gamma\sin\kappa, \cos\gamma)$. This is equivalent to requiring $v_{\hat{k}} \equiv \lim_{|\mathbf{k}|\to 0}\omega_{\mathbf{k}}/|\mathbf{k}| = v_s\sin\gamma\cos(\kappa-\xi) + v_a\sin\gamma\cos\kappa + \sqrt{c^2 + 2v_sv_a\cos\xi + v_a^2\sin^2\gamma\cos^2\kappa} > 0$ for all $\gamma \in [0,\pi]$ and $\kappa \in [0,2\pi)$, which gives the critical value v_s in each fixed direction $\xi \in [0,2\pi)$. The critical velocity calculated here is the so-called $\mathbf{v}_{\text{flow}}$ [25], where the condensate is considered to move with a velocity $\mathbf{v}_s$ with respect to the laser field and impurity. Another kind of critical velocity is defined by a moving impurity inside a static condensate: $\mathbf{v}_{\text{drag}} = \lim_{|\mathbf{k}|\to 0}(\omega_{\mathbf{k}}|_{\mathbf{v}_s=0})/|\mathbf{k}| = \mathbf{v}_a\cdot\hat{k} + \sqrt{c^2 + (\mathbf{v}_a\cdot\hat{k})^2}$. The two are different due to a violation of the Galilean invariance for center-of-mass motion of atoms in the laser field.

In Fig. 2, we show the numerically calculated critical superfluid velocity, $(v_{s,x}/c, v_{s,y}/c, 0)$, where $v_{s,x} \equiv v_s\cos\xi$ and $v_{s,y} \equiv v_s\sin\xi$. Note that there is an axial symmetry along the $\hat{x}$ axis in our system. As one can see, the minimum critical velocity may appear neither along nor perpendicular to $\mathbf{v}_a$, showing a hybridization effect of the synthetic gauge field and superfluidity. This is a clear evidence that the density fluctuation in the gauge potential is coupled to the kinetic energy, and it does not exist if the synthetic gauge field is generated solely by the laser field without interaction.

IV. RESULTS IN A HARMONIC TRAP

Now we solve the static GP equation of Eq. (12) with a harmonic trap $V_{\text{trap}}(\mathbf{r}) = \frac{1}{2}m\omega^2\mathbf{r}^2$. For a 1D trap along the x axis considered in Ref. [17], the gauge field can be eliminated via the transformation $\psi(x) = \psi_0(x)\exp[-i\int_0^x a\rho(x')dx']$. The transformed wave function $\psi_0(x)$ satisfies the conventional GP equation without the gauge field term and therefore can be

well approximated within the Thomas-Fermi approximation (TFA). The resulting ground-state wave function is $\psi(x) = \sqrt{\frac{\mu - m\omega^2 x^2/2}{b}} \exp[-i\frac{a(\mu x - m\omega^2 x^3/6)}{b}]$. Note that the particle current is zero for $v = \frac{1}{m}(-a\rho + a\rho) = 0$, even though the wave function is complex.

For higher dimensional systems, the gauge field cannot be completely gauged away. We start from the following static hydrodynamic equations:

$$0 = -\nabla \cdot \mathbf{j} \equiv -\nabla \cdot (\rho \mathbf{v}), \tag{24a}$$

$$\mu = \frac{-\hbar^2}{2m\sqrt{\rho}}\nabla^2\sqrt{\rho} + \frac{1}{2}m\mathbf{v}^2 + b\rho + \frac{1}{2}m\omega^2\mathbf{r}^2, \tag{24b}$$

where $\mathbf{j}$ is the current density and superfluid velocity $\mathbf{v}_s(\mathbf{r}) = \frac{1}{m}(\nabla\eta + a\rho\hat{x})$ assuming the laser is along the $\hat{x}$ axes. We can get the density function from Eq. (24b) within TFA again by neglecting the kinetic energy term, so that $\mu = m\omega^2 R^2/2$ and $\rho = m\omega^2(R^2 - r^2)/2b$. Here R is the TF radius and determined by the total number of particles. By substituting this density expression in Eq. (24a), we obtain the differential equation of η,

$$-\frac{(R^2 - \mathbf{r}^2)}{2}\nabla^2\eta + r\partial_r\eta = f(\mathbf{r}), \tag{25}$$

where $f(\mathbf{r}) \equiv -am\omega^2 x(R^2 - \mathbf{r}^2)/b$. We first try to solve the eigenequation

$$-\tfrac{1}{2}(R^2 - r^2)\nabla^2\eta + r\partial_r\eta = \epsilon\eta, \tag{26}$$

and then use Green's function method to solve Eq. (25).

A. Coreless vortex-antivortex pair in the 2D trap

For the 2D case, we use the polar coordinate (r,θ) and decompose the phase function into $\eta(r,\theta) = D(r)e^{-il\theta}$, and then Eq. (26) becomes

$$\epsilon D(r) = -\frac{(R^2 - r^2)}{2}\left[D''(r) + \frac{1}{r}D'(r) - \frac{l^2}{r^2}D(r)\right] + rD'(r). \tag{27}$$

Subsequently, we define a new radial function $G(r) = D(r)/r^{|l|}$ and substitute it into the above equation, and then we have

$$\epsilon G(r) = -\frac{(R^2 - r^2)}{2}\left[G''(r) + \frac{2|l| + 1}{r}G'(r)\right] + |l|G(r) + rG'(r). \tag{28}$$

Now, by introducing the new variable $u = r^2/R^2$, we can transform Eq. (28) into a familiar form:

$$0 = u(1-u)G''(u) + [(|l| + 1) - (|l| + 2)u]G'(u) + \frac{\epsilon - |l|}{2}G(u), \tag{29}$$

which is the standard form for the hypergeometric function ${}_2F_1(\alpha,\beta,\gamma;u)$,

$$0 = u(1-u)F''(u) + [\gamma - (\alpha + \beta + 1)u]G'(u) - \alpha\beta G(u). \tag{30}$$

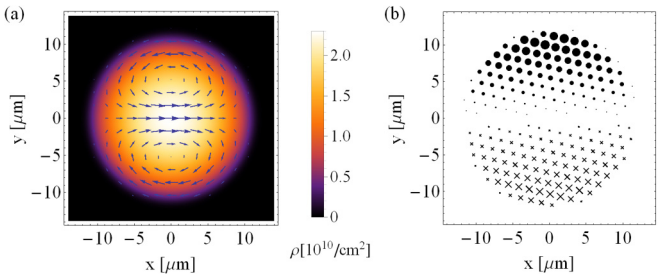

FIG. 3. (Color online) (a) The spatial distribution of particle density (brightness) and current density (arrows) in a 2D harmonic trap. (b) The density-dependent magnetic field $\mathbf{B} = \nabla \times \mathbf{a}\rho$ induced by interaction. Here we use parameters of ^{87}Rb atoms with the two spin states, $|\uparrow\rangle = |F = 2, m_F = +1\rangle$ and $|\downarrow\rangle = |F = 1, m_F = -1\rangle$ [26], trapped in a quasi-2D isotropic harmonic trap with trapping frequency $\omega = 2\pi \times 60$ Hz. We choose total particle number, $N = 5.0 \times 10^4$. The laser beams are along the x direction, i.e., $\mathbf{k}_r = k_r\hat{x}$. The recoiled momentum, $k_r = 2\pi \times 1\mu\text{m}^{-1}$, and $\Omega = 2\pi \times 10$ kHz. Scattering lengths $a_a = 3$ nm and $a_s = 6$ nm are used when near the Feshbach resonance [27–30]. The chemical potential is $\mu \simeq 2\pi \times 2.1$ kHz for a transverse confinement length 0.53 μm.

For the function to be well behaved, it requires $\alpha = -n$, where n is a non-negative integer. By comparing Eq. (29) with Eq. (30), we have $\beta = |l| + n + 1, \gamma = |l| + 1, \epsilon = |l| + 2n + 2n|l| + 2n^2$. Consequently, the eigenfunction of Eq. (26) is $\eta_{nl} = \tilde{C}_{nl}r^{|l|}{}_2F_1(-n, |l| + n + 1, |l| + 1; \frac{r^2}{R^2})e^{-il\theta}$ with eigenvalue $\epsilon_{nl} = |l| + 2n + 2n|l| + 2n^2$. Here, $\tilde{C}_{nl}$ is the normalization coefficient.

Now we can solve Eq. (25) by Green's function method,

$$\eta(\mathbf{r}) = \sum_{n,l}\int d\mathbf{r}'\eta_{nl}(\mathbf{r})\frac{1}{\epsilon_{nl}}\eta^*_{nl}(\mathbf{r}')f(\mathbf{r}') = \frac{am\omega^2 x(r^2 - 3R^2)}{7b}. \tag{31}$$

Actually, only a few components η_{nl} give nonzero contribution in the expansion above. By substituting the ρ and η into the expression of superfluid velocity $\mathbf{v}$, we obtain

$$\mathbf{v} = \frac{2a\omega^2}{7b}(x^2 + R^2/4 - 5r^2/4, xy).$$

In Fig. 3(a), we show the full numerical results of the particle density $\rho(\mathbf{r})$ and the current density $\mathbf{j}(\mathbf{r})$ distribution, which agree with the analytic results (not shown) very well. We note that the ground state has a pair of coreless vortices for the persistent current, and the center of vortices (given by the zero velocity point) is located at $(0, \pm R/\sqrt{5})$. We emphasize that such a coreless vortex can be regarded as a result of a synthetic magnetic field flux, which is induced by the synthetic gauge field [Fig. 3(b)]. Mathematically, $\oint \mathbf{v} \cdot d\mathbf{l} = \int(\nabla \times \mathbf{v}) \cdot d^2\mathbf{r} = \frac{1}{m}\int(\nabla \times \mathbf{a}\rho) \cdot d^2\mathbf{r}$, which supports our claim.

B. Coreless vortex ring in the 3D trap

For the 3D case, there is a detailed calculation of solving differential Eq. (26) in Ref. [31] and the process is similar to the 2D case, so we will not repeat the details here but do show the results. The eigenfunction of Eq. (26) in

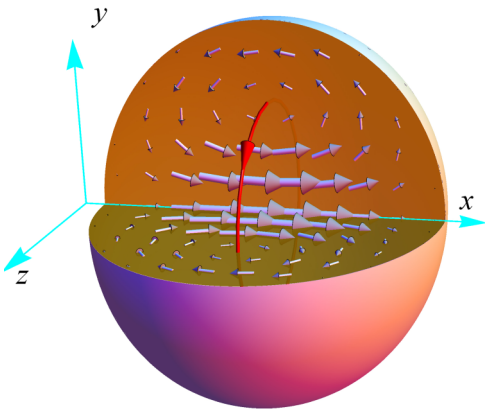

FIG. 4. (Color online) The current (arrows) distribution in a 3D harmonic trap. The parameters are same as in Fig. 3 except for the total particles $N = 1 \times 10^6$ and the 3D trap $(\omega,\omega,\omega) = 2\pi \times (60,60,60)$ Hz. The Thomas-Fermi radius $R = 12.8\,\mu$m and the corresponding chemical potential $\mu \simeq 2\pi\hbar \times 2.5$ kHz. The radius of the coreless ring is 7.4 μm, and the direction on the ring is used to mark the direction of magnetic field $\mathbf{B} = \nabla \times \mathbf{a}\rho$.

3D is $\eta_{nlm} = C_{nl} r^l {}_2F_1(-n, l+n+3/2, l+3/2; \frac{r^2}{R^2}) Y_{lm}$ with eigenvalue $\epsilon_{nlm} = l + 3n + 2nl + 2n^2$. Here C_{nl} is the normalization coefficient. Using the Green's function method, we can get the phase $\eta(\mathbf{r}) = am\omega^2 x(r^2 - 3R^2)/8b$, so that the superfluid velocity is

$$v_{sx} = \frac{a\omega^2}{4b}x^2 + \frac{a\omega^2}{8b}(R^2 - 3r^2), \tag{32}$$

$$v_{sy} = \frac{a\omega^2}{4b}xy, \quad v_{sz} = \frac{a\omega^2}{4b}xz, \tag{33}$$

where the persistent current forms a coreless vortex ring with a radius $R/\sqrt{3}$ around the laser direction. In Fig. 4, we show the current distribution in a 3D trap. We emphasize that the coreless vortex structure here has a length scale of the system size, which is different from the persistent current structure of the stripe phase in the SO regime [32].

V. EXPERIMENT MEASUREMENT

There are several methods to measure the topological condensate proposed in this paper. We first consider a time-of-flight (TOF) measurement, where the two spin components are decoupled and freely expand. In Fig. 5(a), we show the momentum distribution calculated from the condensate in a 2D trapped system. The condensate cloud of the two species is clearly seen to have a constant shift in the momentum distribution with respect to the their recoiled momentum, $\pm k_r$. The shift for each component can be easily calculated to be $\Delta\mathbf{k}_\uparrow \approx \Delta\mathbf{k}_\downarrow \approx \frac{\Delta N}{N}\mathbf{k}_r$ (if $\mu \ll \Omega$), where $\frac{\Delta N}{N} \equiv \frac{N_\uparrow - N_\downarrow}{N} = -\frac{g_a}{3g_s}\frac{\mu}{\Omega} = -\frac{g_a\rho(0)}{3\Omega}$ for the 2D case, and $\frac{\Delta N}{N} = -\frac{2g_a}{7g_s}\frac{\mu}{\Omega} = -\frac{2g_a\rho(0)}{7\Omega}$ for the 3D case within the TFA. Here $\rho(0)$ is the density in the center of the trap. Note that the interaction-induced gauge field can be enhanced by considering Feshbach resonance or confinement resonance. The coreless vortices or vortex ring can be also measurable by interfering with another condensate of no (or different) gauge field.

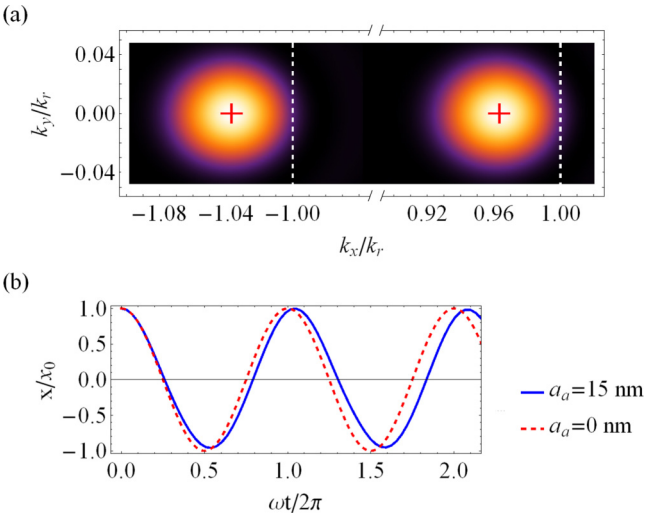

FIG. 5. (Color online) (a) Momentum distribution of a typical condensate shown in Fig. 3, which can be measured in the TOF experiment. Left (right) part is the spin-up (spin-down) component. The vertical dashed line is guiding the position of condensate center without gauge field. (b) The dipolar oscillation of a condensate of total 5×10^3 particles with an initially displaced center at position $(x_0 = 2.8\ \mu\text{m}, 0)$ in a 2D trap of frequency $2\pi \times (240,240)$ Hz. To signify this effect induced by gauge field, we use the parameter $a_a = 15$ nm (solid blue [gray] line), while other parameters are the same as used in Fig. 3.

In the presence of a uniform magnetic field, the celebrated Kohn theorem [19,20] shows that the center-of-mass oscillation frequency should be independent of the interparticle interaction. In a SO-coupled condensate (where the atom-light coupling field is weak), the single-particle dispersion is distorted and the Kohn theorem can fail even *without* interatom interaction [33] or with interaction [34]. In the density-dependent synthetic gauge field we discuss here in the large Ω limitation, however, the Kohn theorem fails to apply *only* when the interaction effect is included. In Fig. 5(b), we show how the oscillation frequency along the $\hat{x}$ direction is changed in the presence of the synthetic gauge field.

VI. SUMMARY

In this paper, we have systematically derived a generalized synthetic gauge field theory for a coupled two-component bosonic system, where the interparticle interaction is included by a self-consistent equation. In the strong interaction regime, we show a Stoner-type ferromagnetism by the interplay of gauge field and interparticle coupling. In the weak interaction limit, we show the anisotropic critical velocity in a uniform space and the topological structure of the persistent currents in a harmonic trap. These distinctive features can be observed in the standard TOF and dipolar oscillation experiments.

ACKNOWLEDGMENTS

We thank M. Cazalilla, Y.-J. Lin, Y.-C. Cheng, and C. S. Chu for fruitful discussions. This work is supported by MoST and National Center for Theoretical Sciences in Taiwan, as well as the European Social Fund under the Global Grant measure.

[1] K. V. Klitzing, G. Dorda, and M. Pepper, Phys. Rev. Lett. **45**, 494 (1980).
[2] D. C. Tsui, H. L. Stormer, and A. C. Gossard, Phys. Rev. Lett. **48**, 1559 (1982).
[3] R. B. Laughlin, Phys. Rev. Lett. **50**, 1395 (1983).
[4] D. R. Hofstadter, Phys. Rev. B **14**, 2239 (1976).
[5] N. Cooper, Adv. Phys. **57**, 539 (2008).
[6] A. L. Fetter, Rev. Mod. Phys. **81**, 647 (2009).
[7] G. Juzeliūnas, J. Ruseckas, P. Öhberg, and M. Fleischhauer, Phys. Rev. A **73**, 025602 (2006).
[8] J. Dalibard, F. Gerbier, G. Juzeliūnas, and P. Öhberg, Rev. Mod. Phys. **83**, 1523 (2011).
[9] N. Goldman, G. Juzeliūnas, P. Öhberg, and I. B. Spielman, Rep. Prog. Phys. **77**, 126401 (2014).
[10] Y.-J. Lin, R. L. Compton, and K. Jimenez-Garcia, J. V. Porto, and I. B. Spielman, Nature (London) **462**, 628 (2009).
[11] I. B. Spielman, Phys. Rev. A **79**, 063613 (2009).
[12] Y.-J. Lin, K. Jiménez-García, and I. B. Spielman, Nature (London) **471**, 83 (2011).
[13] X.-J. Liu, M. F. Borunda, X. Liu, and J. Sinova, Phys. Rev. Lett. **102**, 046402 (2009).
[14] M. Kiffner, W. Li, and D. Jaksch, Phys. Rev. Lett. **110**, 170402 (2013).
[15] M. Kiffner, W. Li, and D. Jaksch, J. Phys. B: At., Mol. Opt. Phys. **46**, 134008 (2013).
[16] A. Cesa and J. Martin, Phys. Rev. A **88**, 062703 (2013).
[17] M. J. Edmonds, M. Valiente, G. Juzeliūnas, L. Santos, and P. Öhberg, Phys. Rev. Lett. **110**, 085301 (2013).
[18] M. Edmonds, M. Valiente, and P. Öhberg, arXiv:1408.6886.
[19] W. Kohn, Phys. Rev. **123**, 1242 (1961).
[20] S. K. Yip, Phys. Rev. B **43**, 1707 (1991).
[21] H. Zhai, Int. J. Mod. Phys. B **26**, 1230001 (2012), and its references.
[22] S. Sinha, R. Nath, and L. Santos, Phys. Rev. Lett. **107**, 270401 (2011).
[23] T.-L. Ho and S. Zhang, Phys. Rev. Lett. **107**, 150403 (2011).
[24] R. M. Wilson, B. M. Anderson, and C. W. Clark, Phys. Rev. Lett. **111**, 185303 (2013).
[25] W. Zheng, Z.-Q. Yu, X. Cui, and H. Zhai, J. Phys. B: At. Mol. Opt. Phys. **46**, 134007 (2013); Q. Zhu, C. Zhang, and B. Wu, Europhys. Lett. **100**, 50003 (2012); T. Ozawa, L. P. Pitaevskii, and S. Stringari, Phys. Rev. A **87**, 063610 (2013).
[26] D. M. Stamper-Kurn and M. Ueda, Rev. Mod. Phys. **85**, 1191 (2013).
[27] P. O. Fedichev, Y. Kagan, G. V. Shlyapnikov, and J. T. M. Walraven, Phys. Rev. Lett. **77**, 2913 (1996).
[28] M. Theis, G. Thalhammer, K. Winkler, M. Hellwig, G. Ruff, R. Grimm, and J. H. Denschlag, Phys. Rev. Lett. **93**, 123001 (2004).
[29] K. Enomoto, K. Kasa, M. Kitagawa, and Y. Takahashi, Phys. Rev. Lett. **101**, 203201 (2008).
[30] D. J. Papoular, G. V. Shlyapnikov, and J. Dalibard, Phys. Rev. A **81**, 041603 (2010).
[31] C. Pethick and H. Smith, *Bose-Einstein Condensation in Dilute Gases*, 2nd ed. (Cambridge University Press, New York, 2008), Chap. 7.
[32] T. Ozawa and G. Baym, Phys. Rev. A **85**, 063623 (2012).
[33] E. van der Bijl and R. A. Duine, Phys. Rev. Lett. **107**, 195302 (2011).
[34] Y. Li, G. I. Martone, and S. Stringari, Europhys. Lett. **99**, 56008 (2012).